Journal of Alloys and Compounds 481 (2009) 600–604

Contents lists available at ScienceDirect

Journal of Alloys and Compounds

journal homepage: www.elsevier.com/locate/jallcom

Synthesis of nano-crystalline spherical cobalt–iron (Co–Fe) alloy particles by ultrasonic spray pyrolysis and hydrogen reduction

Sebahattin Gurmen[a,*], Aybars Guven[a], Burcak Ebin[a], Srećko Stopić[b], Bernd Friedrich[b]

[a] Istanbul Technical University, Metallurgical & Materials Eng. Dept., 34469 Istanbul, Turkey
[b] IME Process Metallurgy and Metal Recycling, RWTH Aachen University, Germany

ARTICLE INFO

Article history:
Received 16 September 2008
Received in revised form 9 March 2009
Accepted 10 March 2009
Available online 20 March 2009

Keywords:
Nanostructured materials
Metals and alloys
Co–Fe
Ultrasonic spray pyrolysis

ABSTRACT

Spherical nano-crystalline Co–Fe particles were produced by ultrasonic spray pyrolysis (USP) of aqueous solutions of cobalt–iron chloride followed by thermal decomposition of generated aerosols in hydrogen atmosphere. The effect of the precursor solution in the range of 0.05 M, 0.1 M, 0.2 M and 0.4 M on the morphology and crystallite size of the Co–Fe alloy particles are investigated under the conditions of 1.5 h running time, 800 °C reduction temperature, and 1.0 l/min H_2 volumetric flow rate. X-ray diffraction (XRD) studies and Scherer crystallite size calculations show that the crystallite size varies between 25 nm and 27 nm. Scanning electron microscopy (SEM) observations reveal that the the precursor solution strongly influences the particle size of the synthesized Co–Fe alloy particles. Energy dispersive spectroscopy (EDS) results indicate that particles consist of iron and cobalt. Spherical nano-crystalline Co–Fe alloy particles in the range of 100–920 nm were obtained at 800 °C.

1. Introduction

Nanoscale particle research has recently become a very important field in materials science. Such metal nanoparticles often exhibit very interesting electronic, magnetic, optical, and chemical properties. Their unique features depend on their size, shape, surface composition, and surface atomic arrangement [1–5]. Magnetic nanoparticles have received a great deal of attention from both basic research and technological applications. Of all the magnetic materials such as metal oxides and pure metals, cobalt and iron are representative for their excellent magnetism. Especially, cobalt is found an important element which is used as additional component to improve the coercivity of the material. For example, Fe–Co alloys possess a much higher coercivity than that of pure iron [6]. Conventional Fe–Co alloys are important soft magnetic materials that have been widely and commercially used in industry. Nanocomposite soft magnetic materials are expected to be useful for high frequency and high temperature operation, in contrast to conventional ferrites, which exhibit poor magnetic properties at high frequencies and elevated temperatures. Furthermore, magnetic materials are of key importance in microwave absorbing materials that are being applied in the classified stealth technology. Thus, the synthesis and characterization of efficient and high performance nanomagnetic materials have become more and more important [7,8]. Spherical non-agglomerated submicron particles of complex composition and controlled phase content, suitable for direct application or fabrication of high technology sintered materials, can be prepared by the spray pyrolysis method [9]. The USP is a versatile technique for producing various materials in a wide range of composition, size and morphology. USP of solutions is performed by applying a powerful source of ultrasound to the corresponding solution forming an aerosol with constant droplet size, which depends on the characteristic of the liquid and the frequency of the ultrasound. At a resonance frequency of the order of 2 MHz, the droplet size is approximately 2 μm [10]. Ultrasonic spray pyrolysis enables the subsequent reactions to occur in a very small volume leading to an ultra fine powder. The different form of produced particles is present due to the process conditions leading to either volume or surface precipitation within the droplet and the subsequent conversion to a dense, solid particle or one hollow, shell-like particle. From the viewpoint of the application of the as-generated particles for advanced materials synthesis, particle morphology has great interest. It is presumed that certain particle morphology is formed during the evaporation/drying stage that encountered processes of evaporation and diffusion of both the solvent and solute, changing in droplet temperature and crust formation. Messing et al. [11] mentioned that developments in process control, atomisation, and system design are required for wider commercialisation of spray pyrolysis process. USP is a useful tool for large-scale or small-scale production of particles with controlled particle size. The fabrication of CoFe nanoparticles in this way has not yet been investigated. And only a few studies for the synthesis of iron–cobalt particles by gas phase chemical reaction have been reported in the literature [12–18]. Fe–Co alloyed nanoparticles were produced by chemical vapor con-

* Corresponding author.
E-mail address: gurmen@itu.edu.tr (S. Gurmen).

0925-8388/$ – see front matter © 2009 Elsevier B.V. All rights reserved.
doi:10.1016/j.jallcom.2009.03.046

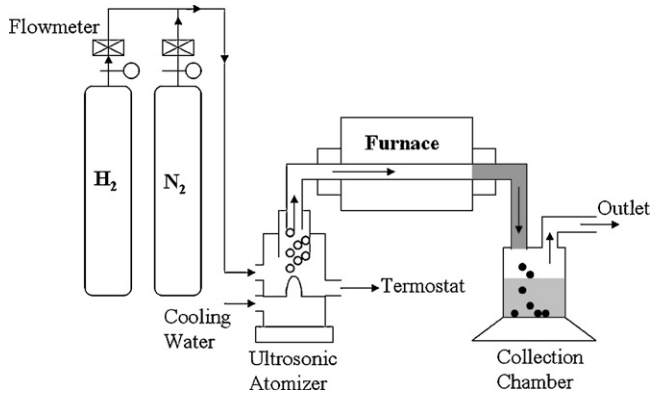

Fig. 1. Schematic drawing of experimental apparatus for the synthesis of Co–Fe nanoparticles.

densation using organomatellic iron carbonyl ($Fe(CO)_5$) and cobalt carbonyl ($Co_2(CO)_8$) as precursors by Wang et al. [13]. Nano-sized Fe–Co alloy powders were synthesized by chemical solution mixing of metal salts and hydrogen reduction [14]. Poddar et al. [15] report on the magnetic properties of Fe–Co nanocomposites synthesized using the microwave plasma technique. Multifunctional Fe–Co nanoparticles with narrow size distribution were fabricated by a novel physical vapor nanoparticle-deposition technique by Xu et al. [16]. Ferromagnetic metallic nanoparticles were produced by laser evaporation with vapor condensation in an aggregation gas by Morasa et al. [17]. Soft-magnetic Fe–Co alloy nanoparticles with diameters less than 100 nm are prepared by ball milling. Yu et al. [18] applied the USP technique to synthesize carbon-encapsulated magnetic nanoparticles.

A novel route to prepare nano-crystalline spherical cobalt–iron (Co–Fe) alloy particles via USP using a leach solution of $CoCl_2$ und $FeCl_2$ as precursors will be investigated. The effects of the processing parameters on their size and microstructure were characterized via X-ray diffraction (XRD), and scanning electron microscopy (SEM).

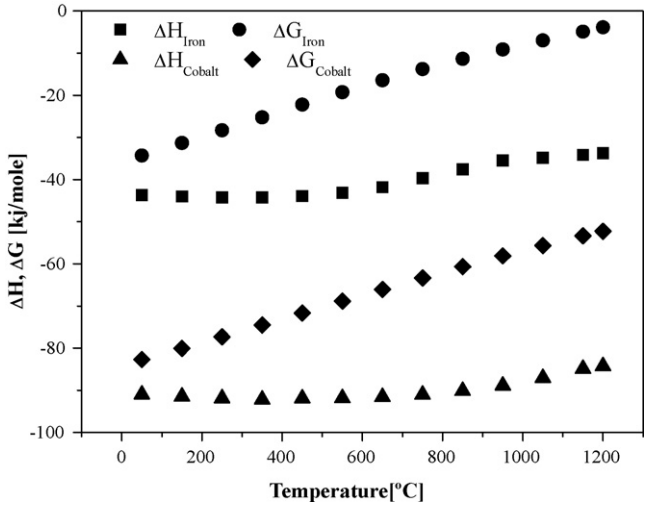

Fig. 2. Dependence of the Gibb's energy on the temperature.

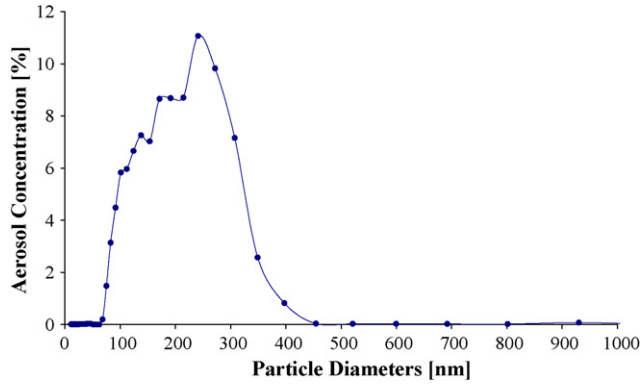

Fig. 3. Typical particle size classification in a carrier gas (precursor solution: 0.05 M $CoCl_2{\cdot}6H_2O + FeCl_2{\cdot}4H_2O$, carrier gas: N_2).

2. Experimental

2.1. Materials

All the reagents ($CoCl_2{\cdot}6H_2O$ and $FeCl_2{\cdot}4H_2O$) were analytical grade and used without further purification. A water leach solution of $CoCl_2{\cdot}6H_2O$ and $FeCl_2{\cdot}4H_2O$ (powders were dissolved in deionized water for mixing of the salts) was used as starting material for this research. The deionized water (resistivity $\rho > 18\,M\Omega$) was used for all solutions. The concentration of the precursor solution is between 0.05 mol/l and 0.4 mol/l. All solutions were stirred for 1 h using a magnetic stirrer.

2.2. Experimental procedure

The nano-crystalline spherical Co–Fe alloy particles were synthesized using the ultrasonic spray pyrolysis method. Fig. 1 shows the schematics of the apparatus. The experiments were done at 800 °C starting from cobalt–iron chloride solutions with concentrations of 0.05 mol/l and 0.4 mol/l. Very fine droplets of the aerosol were obtained in an ultrasonic atomizer Pyrosol 7901 (Ramine Baghai Instrumentation, with a frequency of 2.1 MHz). The aerosol was transported by H_2-carrier/reduction gas via a quartz tube (0.7 m length and 0.02 m diameter) to an electrical heated furnace (Ströhlein, Germany) with a temperature control of ±1 °C. Because of the safety reasons and to create an inert atmosphere, nitrogen with a flow rate of 1 l/min was used prior to the reduction process. Under spray pyrolysis conditions in hydrogen atmosphere and at a flow rate of 1 l/min, the dynamic (continuous) reduction took place in the quartz tube reactor (heated zone 280 mm). The residence time, calculated from the ratio of the volume of the reaction zone and the carried gas flow, was about 5.3 s with the assumption that the rate of droplets and the carried gas are equal. According to model one particle from one droplet [10] we supposed that this short reaction time is sufficient for the transformation of droplets to metal particle in the hydrogen atmosphere. A particle size classifier (Different Mobility Analyzer, Vienna-Type Model 5.500) was used for the size distribution of droplets suspended in a carrier gas. An X-ray diffractometer (Phillips PW 1700), transmission electron microscope (JEOL 2000 EX) and scanning electron microscope (Zeiss DSM 982 Gemini) were used for the characterization of the obtained Co–Fe powders. The chemical compositions of particles were investigated by the EDS analyses. For XRD analysis, the Co–Fe dispersed particles were placed on a glass substrate and allowed to dry in air at room temperature. SEM images were used to observe the surface morphology of particles formed at different reaction temperatures. The powders were first dispersed in ethanol and inserted in ultrasonic bath for 30 min and then the suspension was dispersed dropwise onto a glassy carbon slide to make a thick film, which later coated by palladium for SEM characterization.

Table 1 contains data for chemical composition of the applied solutions, conditions of the production process, and a short description of the obtained powders.

Table 1
Composition of precursor solutions, conditions of the process, and descriptions of the obtained powders ($T_{precursor}$ = 25 °C, test period = 1.5 h, volume of used solution = 340 ml).

No	Concentration of precursor solution (mol/l)	Temperature (°C)	Flow rate of H_2 (l/min)	Characteristic of the product
1	0.05 M ($CoCl_2{\cdot}6H_2O + FeCl_2{\cdot}4H_2O$)	800	1	Spherical, nano-structured cobalt–iron powder
2	0.1 M ($CoCl_2{\cdot}6H_2O + FeCl_2{\cdot}4H_2O$)	800	1	Spherical, nano-structured cobalt–iron powder
3	0.2 M ($CoCl_2{\cdot}6H_2O + FeCl_2{\cdot}4H_2O$)	800	1	Spherical, nano-structured cobalt–iron powder
4	0.4 M ($CoCl_2{\cdot}6H_2O + FeCl_2{\cdot}4H_2O$)	800	1	Spherical, nano-structured cobalt–iron powder

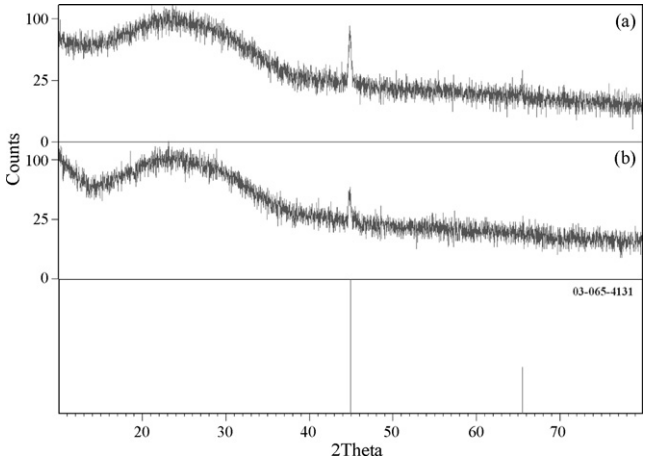

Fig. 4. X-ray analysis of the USP-HR Co–Fe particles: (a) 0.4 M $CoCl_2{\cdot}6H_2O + FeCl_2{\cdot}4H_2O$, 800 °C, (b) 0.05 M $CoCl_2{\cdot}6H_2O + FeCl_2{\cdot}4H_2O$, 800 °C.

3. Results and discussion

3.1. Thermodynamic analysis of hydrogen reduction

The reaction for the formation of Co–Fe metal from cobalt–iron chloride can be described as in Eq. (1).

$$CoCl_2 + FeCl_2 + 2H_2 \rightarrow CoFe + 4HCl \quad (1)$$

The thermodynamic analysis is done using Fact-Sage Software and in the temperature range of 50–1200 °C (Fig. 2).

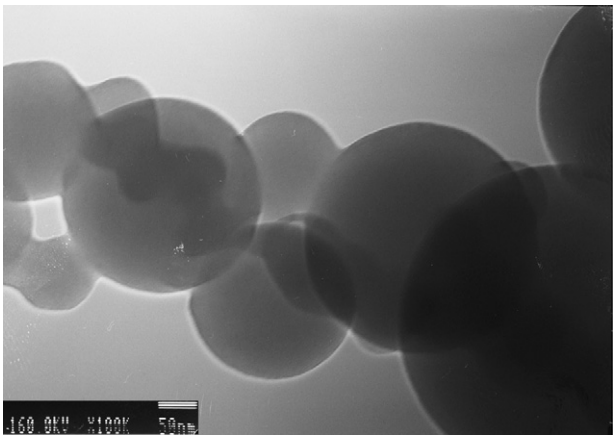

Fig. 6. TEM micrograph of Co–Fe particles produced from 0.05 M precursor.

The values of Gibb's free energy (ΔG°) for the reaction (1) in the temperature range up to 1000 °C confirm the probability for formation of Co–Fe from $CoCl_2 + FeCl_2$ by hydrogen reduction. Although Gibbs free energy is always negative between the 0 and 1200 °C temperature range, it increases through the positive values at elevated temperatures.

3.2. Differential Mobility Analyzer (DMA) of aerosol

In a typical spray pyrolysis process, an aqueous solution of precursors is atomized and the stream consisting of droplets suspended in a carrier gas is classified (analyzed) via DMA. Fig. 3 shows the size distribution of droplets suspended in a carrier gas with aerosol concentration.

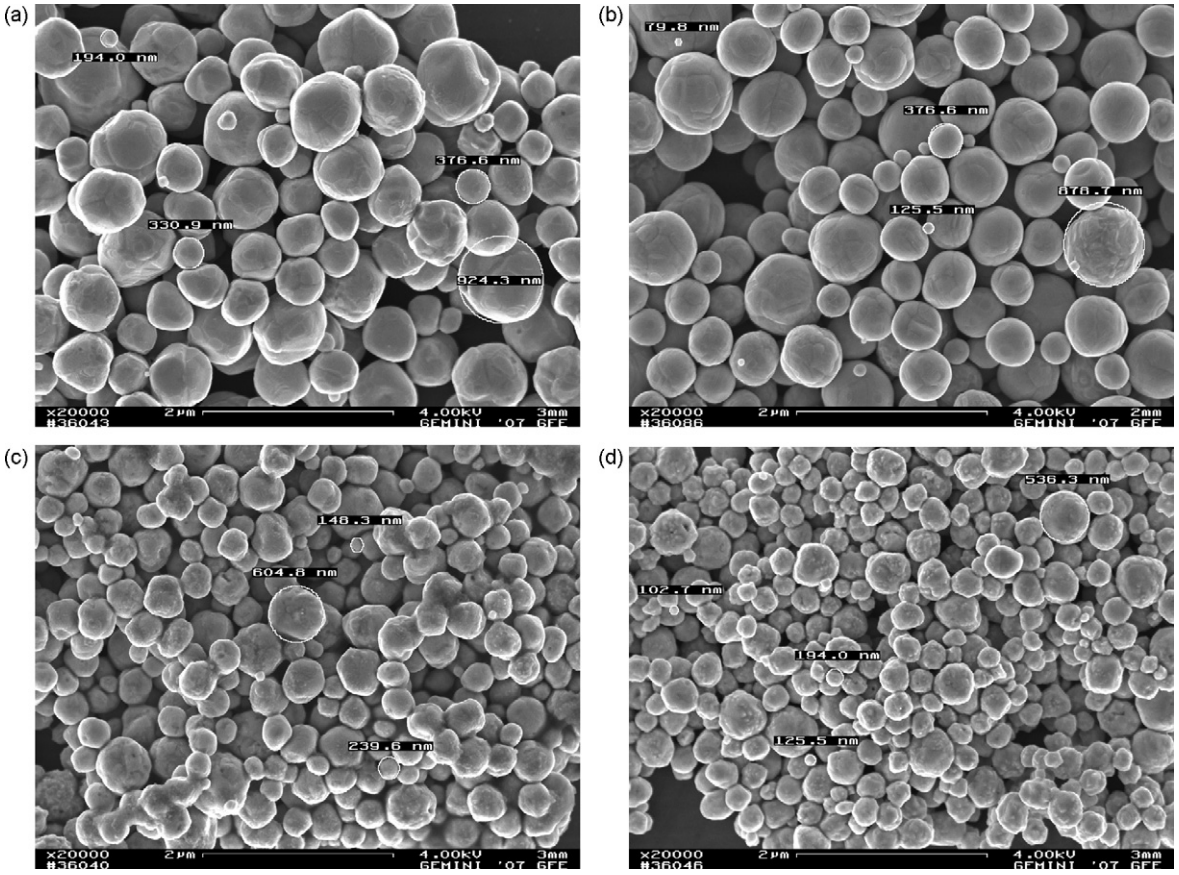

Fig. 5. SEM images of Co–Fe particles prepared at 800 °C with different precursor concentration. (a) 0.4 M, (b) 0.2 M, (c) 0.1 M and (d) 0.05 M.

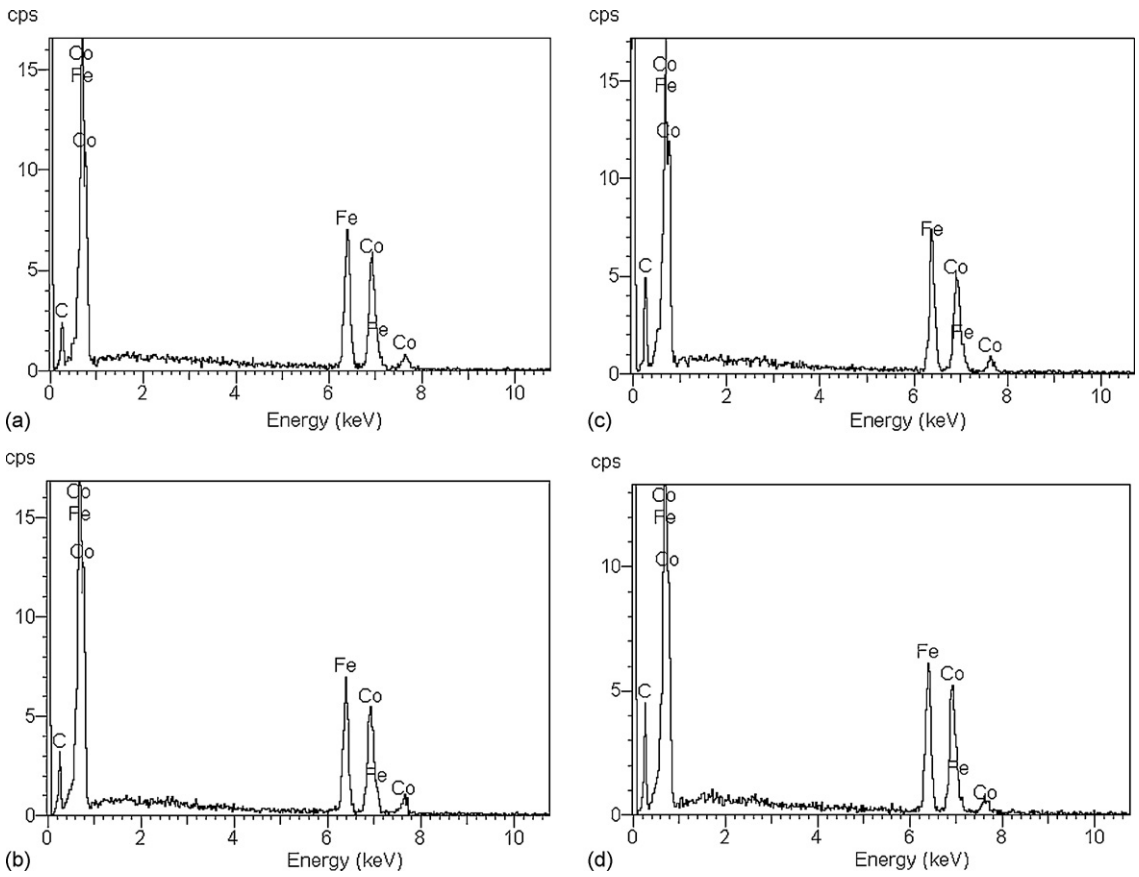

Fig. 7. EDS results of Co–Fe particles obtained from (a) 0.4 M, (b) 0.2 M, (c) 0.1 M and (d) 0.05 M precursor concentrations.

As seen from Fig. 3, the aerosol concentration is 0.236% for the particle diameter range of 11–62 nm; 99.554% for 68–397 nm; and 0.209% for 454–930 nm.

3.3. X-ray analysis of Co–Fe particles

Fig. 4 shows X-ray diffraction (XRD) patterns of the USP-HR Co–Fe particles. The body centered cubic crystalline Co–Fe phase has two main peaks at the diffraction angles of 45° and 65°. In Fig. 4, a diffraction peak was observed at 45°. The broad hump at the low diffraction angles are coming from glass substrate which is amorphous. The X-ray analysis of the powders indicated the presence of body centered cubic crystalline structured Co–Fe (JPDS card no: 03-065-4131) nanoparticles and any diffraction peaks due to oxides phases of Co–Fe were not observed.

Crystallite size calculated from XRD patterns by using Scherrer Equation,

$$t = \frac{K\lambda}{B\cos\theta} \quad (2)$$

defines a simple relationship between crystallite size and peak width. In this equation K is constant which value is between 0.85 and 0.9, λ the wavelength of the X-ray (Cu $K\alpha_1$ = 1.541874 Å), B the width (in radians) of the peak due to size effect, θ the Bragg angle, and t is the particle size. The calculated sizes of Co–Fe crystallites for Fig. 4a and b were approximately 25 nm and 27 nm, respectively.

3.4. The effect of precursor solution concentration

In this research the effect of the precursor concentration in the range of 0.05 M, 0.1 M, 0.2 M and 0.4 M was investigated under the conditions of 1.5 h running time, 800 °C reduction temperature, and 1.0 l/min H_2 volumetric flow rate. SEM images of the obtained Co–Fe particles are shown in Fig. 5.

The SEM micrographs show the typical morphology of Co–Fe alloy particles. The shape of the particles is nearly spherical with homogeneous size distribution. Co–Fe alloy particles in the range of 100–920 nm were prepared by using 0.4 M precursor concentration (see Fig. 5a). However decrease of the concentration in the precursor solution (from 0.4 M to 0.2 M, and 0.1 M and 0.05 M) cause the reducing in the mean particle diameter from 630 nm to 490 nm, and 310 nm, and increase the uniformity under the same synthesis conditions (in Fig. 5b and c). Obtained smallest particle size was 100 nm under the 0.05 M precursor concentration (see Fig. 5d). In Fig. 5d the size of the Co–Fe particles varies between 100 nm and 600 nm. Also, the SEM investigations revealed that some of the particles were formed by agglomeration of the smaller particles. TEM micrograph (Fig. 6) of Co–Fe particles obtained from 0.05 M solution proves that particles have totally spherical and dense structure.

The EDS results (Fig. 7) indicate that particles synthesized from all solution concentrations contain iron and cobalt. Carbon peaks in the results exist due to substrate which is glassy carbon slide. Besides that, there is no impurity observed in the chemical composition of the particles caused by other reaction products such as chlorine. Also, EDS analysis indicate that atomic percents of the cobalt and iron are same (Co/Fe = 1/1) for all of the particles.

4. Conclusion

Nano-crystalline Co–Fe alloy particles have been synthesized via USP-HR. The effect of the precursor solution in the range of 0.05 M, 0.1 M, 0.2 M and 0.4 M on the morphology and crystallite size of the Co–Fe alloy particles are investigated under the conditions of 1.5 h running time, 800 °C reduction temperature, and 1.0 l/min H_2

volumetric flow rate. The X-ray analysis of the powders indicated the presence of body centered cubic crystalline structured Co–Fe nanoparticles. From XRD analysis, it is found that the crystallite size of the Co–Fe alloy particles are 25 and 27 nm for 0.05 M and 0.4 M precursors, respectively. The experimental results confirmed that the decrease of the concentration of precursor solution decreases the mean particle size from 920 nm to 100 nm. In all cases, dense Co–Fe particles show almost spherical morphology, homogeneous size distribution and smooth surface. Moreover, particles consist of iron and cobalt in homogeneous composition distribution.

Acknowledgments

We would like to thank the Alexander von Humboldt Foundation for providing research fellowships to Dr. Sebahattin Gürmen allowing 2-month stay at the IME Process Metallurgy and Metal Recycling, RWTH Aachen University. Also we would like to thank Mr. Dieter Leimbach for his highly motivated assistance in our experimental part.

References

[1] B. Zhou, S. Hermans, S. Somorjai, Nanotechnology in Catalysis, Kluwer Academic/Plenum Publishers, New York, 2004, pp. 361–399.
[2] R.W. Siegel, Nanophase Materials: Synthesis, Structure, and Properties, Springer-Verlag, 1994.
[3] V. Jokanovic, in: A.M. Spasic, J.P. Hsu (Eds.), Nanodesigning Surfactant Science Series 130, CRC Press, Taylor& Francis Group, Boca Raton, 2006, pp. 513–533.
[4] S. Stopić, P. Dvorak, B. Friedrich, World of Metallurgy – Erzmetall 58 (2005) 195–201.
[5] Z.H. Wang, C.J. Choi, B.K. Kim, J.C. Kim, Z.D. Zhang, J. Alloy Compd. 351 (2003) 319–323.
[6] D. Yang, X. Ni, D. Zhang, H. Zheng, J. Cheng, P. Li, J. Cryst. Growth 286 (2006) 152–155.
[7] X. Gao, S.C. Tan, A.T.S. Wee, J. Wu, L. Kong, X. Yu, H.O. Moser, J. Electron. Spectrosc. 150 (2006) 11–14.
[8] D.L. Peng, Y. Chen, H. She, R. Katoh, K. Sumiyama, J. Alloy Compd. 469 (2009) 276–281.
[9] S. Gürmen, S. Stopic, B. Friedrich, Mater. Res. Bull. 41 (2006) 1882–1890.
[10] J.H. Kim, V.I. Babushok, T.A. Germer, G.W. Mulholland, S.H. Ehrman, J. Mater. Res. 18 (2003) 1614–1622.
[11] G.L. Messing, S.C. Zhang, G.V. Jayanthy, J. Am. Ceram. Soc. 76 (1993) 2707–2726.
[12] H.D. Jang, D.W. Hwang, D.P. Kim, H.C. Kim, B.Y. Lee, I.B. Jeong, Mater. Res. Bull. 39 (2004) 63–70.
[13] Z.H. Wang, C.J. Choi, J.C. Kim, B.K. Kim, Z.D. Zhang, Mater. Lett. 57 (2003) 3560–3564.
[14] B.-H. Lee, Y.J. Lee, K.H. Min, D.-G. Kim, Y.D. Kim, Mater. Lett. 59 (2005) 3156–3159.
[15] P. Poddar, J.L. Wilson, H. Srikanth, B.G. Ravi, J. Wachsmuth, T.S. Sudarshan, Mater. Sci. Eng. B 106 (2004) 95–100.
[16] Y.H. Xu, J. Bai, J.-P. Wang, J. Magn. Magn. Mater. 311 (2007) 131–134.
[17] K. Morasa, R. Schaarschucha, W. Riehemanna, S. Zinovevab, H. Modrowb, D. Eberbeckc, J. Magn. Magn. Mater. 293 (2005) 119–126.
[18] F. Yu, J.N. Wang, Z.M. Sheng, L.F. Su, Carbon 43 (2005) 3002–3039.